PAGEOPH, Vol. 148, Nos. 1/2 (1996)

0033–4553/96/020021–18$1.50 + 0.20/0

Hybrid Seismic Modeling Based on Discrete-wave Number and Finite-difference Methods

JIŘÍ ZAHRADNÍK[1] and PETER MOCZO[2]

Abstract—Any calculation of seismic wave propagation comprising the seismic source, the travel path, and the receiver site in a single finite-difference (FD) model requires a considerable amount of computer time and memory. Moreover, the methods currently available for including point sources in the 2D FD calculations are far-field approximations only. Therefore we have developed a new hybrid method for treating the seismic wave fields at localized 2D near-surface structures embedded in a 1D background medium, and excited by a point source. The source radiation and propagation in the background model is solved by the discrete-wave number (DW) method, while the propagation in the local 2D structure is calculated by the FD method. The coupling between the two sets of calculations is performed on a rectangular excitation box surrounding the local structure. We show the usefulness of the method in ground-motion studies where both near-field source effects and local site effects are important. Technical problems connected with the inconsistency between the 3D source radiation and the 2D FD calculation are minor for the relatively distant in-plane point explosive sources, but are more serious for the in-plane dislocation sources.

Key words: Seismic waves, strong ground motions, discrete-wave number method, finite-difference method, hybrid method.

Introduction

Modeling of seismic wave fields requires efficient numerical methods. However, efficiency of a particular method is usually restricted to a particular aspect of the wave field. Therefore, it is often advantageous to combine different methods. Such 'hybrid methods' have been developed, for example, by VAN DEN BERG (1984), KUMMER *et al.* (1987), EMMERICH (1992), FÄH *et al.* (1994), and ROVELLI *et al.* (1994). These approaches are based on the combination of finite-element or finite-difference methods with, respectively, analytical methods, the frequency-wave number filter method, the modal summation method, and the stochastic method.

[1] Department of Geophysics, Faculty of Mathematics and Physics, Charles University, V Holešovičkách 2, 180 00 Praha, Czech Republic.

[2] Geophysical Institute, Slovak Academy of Sciences, Dúbravská cesta 9, 842 28 Bratislava, Slovak Republic.

Our intention is to develop a new hybrid method able to treat localized near-surface 2D structures embedded in (possibly deep) 1D media, and excited by relatively distant point sources of arbitrary focal mechanisms. For this purpose we combine the Discrete-Wave number (DW) method and the Finite-Difference (FD) method. Both techniques allow the computation of the complete wave fields, including all body and surface waves, and near-field source effects. The linear stress-strain relation is assumed. The methods can take into account causal attenuation in the form of an arbitrary frequency dependence of the quality factor Q. Large 1D models (i.e., distant sources, and deep models) are relatively easy to tackle for the DW method, but difficult for the FD method. 2D near-surface heterogeneities, on the other hand, are relatively easy for FD, but more difficult for DW. Also point sources are rather difficult to model for pure 2D FD methods, although an approximate transformation between the line and point source is available (VIDALE and HELMBERGER, 1987). This is why we suggest use of the DW method to compute the 1D background wave field. Then, locally, around a 2D near-surface structure, the FD method must be used. The DW-FD coupling is realized similarly to the algorithm of ALTERMAN and KARAL (1968).

Our method most closely resembles that of FÄH *et al.* (1994), who combined the Modal Summation (MS) and the FD approach. Their method has proved successful in many practical applications in earthquake seismology, including those with very complex crustal models. The completeness of the wave field in the MS method, i.e., body phases and near-field effects, can be guaranteed after certain modifications (FÄH, personal communication). Regardless, using DW instead of MS is an innovation, since DW does *automatically* describe the complete wave field, including the near-field effects. Also, our algorithm of the DW-FD coupling is different from the one used by FÄH *et al.* (1994), allowing shallower (i.e., less expensive) FD models. Another contribution of this paper is that we analyze thoroughly the accuracy of the hybrid method. The cases of explosive and dislocation sources are discussed separately, and their different numerical performance is theoretically explained. All examples have a methodical character. Applications to real data will be published elsewhere.

Method

DW method. The DW method (BOUCHON, 1981) is based on an assumed periodic repetition of the sources in a horizontal plane. The periodicity simplifies the integral representation of the elastic wave field in a 1D medium to an infinite summation over horizontal wave numbers. The sum is convergent (i.e., it can be truncated) except in the case in which the receiver and the source have the same depth. For 1D models represented by homogeneous layers the method is combined with the matrix algorithm of KENNETT and KERRY (1979). No principal limitations

are imposed on the source-to-receiver distance, model depth or velocity contrast. The only requirement is that a finite frequency bandwidth and a finite time window are considered.

The causal attenuation (frequency independent Q) is introduced by means of complex valued elastic parameters in the frequency domain, where the Green's tensor is calculated. After multiplication with the seismic moment tensor (prescribing the spectral content and the focal mechanism of the source) and application of the inverse Fourier transform, the time-domain solution is obtained. As long as the source periodicity length is chosen to be large enough and a small amount of an artificial attenuation—later removed from the final solution—is added to prevent time-domain aliasing, the final seismograms are free of any fictitious arrivals. It should be mentioned that the same artificial attenuation also prevents the occurrence of numerical singularities. Successful applications of the DW method require a careful choice of the time- and frequency-window lengths, and their careful sampling, so as to ensure that the results are not affected by aliasing and/or frequency truncation. In this paper the DW method encoded by COUTANT (personal communication, 1994) is used.

FD method. The FD method provides a direct numerical solution of the 2D elastodynamic equations of motion on a finite-extent space domain. The top boundary of the domain is a flat free surface, the others are artificial 'nonreflecting' (or, say, 'transparent') boundaries. Their particular realization is of little interest for this paper. The free-surface and internal grid points of the FD domain are solved by the PS2 scheme developed in ZAHRADNÍK (1995a), and verified for both body and surface waves in ZAHRADNÍK and PRIOLO (1995). The scheme belongs to the so-called heterogeneous schemes, in which the interface continuity conditions are automatically approximated. The free-surface condition is simulated using the so-called vacuum formalism (ZAHRADNÍK *et al.*, 1993). As the PS2 scheme is only 2nd-order accurate, the minimum shear wavelength must be sampled at least at 10–20 grid points in the FD calculation. Optionally, a line (2D) source is included after ABOUDI (1971).

Implementation of the attenuation is based on the approach suggested for SH waves by EMMERICH and KORN (1987), and is equivalent to EMMERICH'S (1992) generalization for the P-SV case. The corresponding equations of motion contain additional terms. Each of these terms obeys an ordinary differential equation. The method makes it possible to account for both an arbitrary frequency dependence of Q, and a spatially varying attenuation. See also MOCZO and BARD (1993).

DW-FD coupling. The DW-FD coupling represents a key point of the hybrid method. Therefore, it is to be described here in a greater detail. Although the algorithm is similar to the one by ALTERMAN and KARAL (1968), three of its features require a good explanation: It is the definition of the excitation and residual wave field, the preferred form of excitation lines, and the interpolation at these lines.

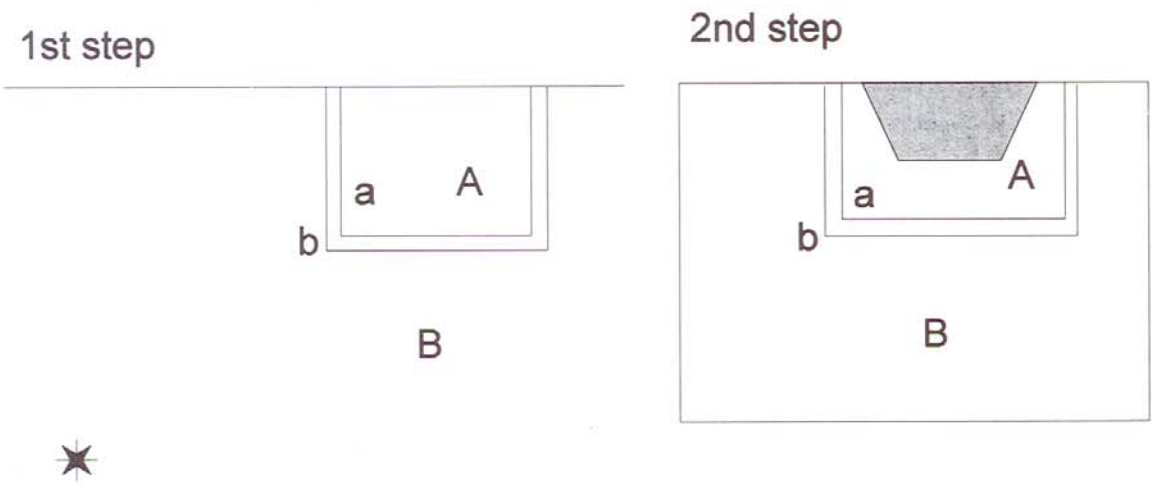

Figure 1
Schematic representation of the hybrid method. In the first step, the source (asterisk) is present in the background medium. The known background wave field U_k is stored along the lines a and b. In the second step, the source is already absent, but a local structure is (optionally) placed inside the excitation box, formed by the lines a and b. Then, the complete wave field $U = U_k + U_r$, and the residual field U_r are computed in the domains A and B, respectively. The top line is the free surface. In the second step the domain B is limited by the left, right and bottom artificial ('nonreflecting') boundaries.

The FD domain is divided in two parts, A, and B, as shown in Figure 1. The lines a and b, belonging to A and B, respectively, are called the excitation lines. Their spacing is equal to the FD grid step. Zone A is the excitation box. The (vector) wave field U is assumed to be represented by

$$u = U_k + U_r, \tag{1}$$

where U_k and U_r are a known and residual part, respectively. The U_k is the wave field corresponding to the 1D medium with no additional local 2D heterogeneity, i.e., the so-called background field. At the excitation lines the part U_k must be known throughout the entire time window computed by the FD method. In zone A the complete field U is computed, while only the residual field U_r is computed in zone B. When calculating U at line a, the required values of U at line b are not directly available from the FD calculation (since only U_r is computed there). Nevertheless, the values of U at line b can be obtained from U_r by adding the known value of U_k. A quite similar approach is employed to calculate U_r at line b. We note that two lines correspond to the 2nd-order FD method. For example, a 4th-order method would require four lines, etc.

Though the U_k values must be at our disposal at the excitation lines a and b for all grid points and all time levels, all these values are not necessarily computed by the DW method and stored there. It is possible to compute and store U_k at relatively coarse irregular positions along the lines a and b, and then make a linear

interpolation into the FD grid points and time levels. This feature of our algorithm is essential for most model configurations. It is because, when treating near-surface (low-velocity) structures by the FD method, relatively small space and time grid steps are to be chosen to control accuracy and stability, respectively. Calculating and storing the DW background solution at such a fine grid would be highly excessive. Moreover, it would be very difficult, or even impossible, to obtain the same time step in the DW and FD method, as both are determined by quite different criteria. Even more important is the possibility of circumventing the convergency problems of the DW method when the source and receiver are at the same depth. At that time we can simply use the receivers above and below the source level, and interpolate between them.

The sampling is at least two locations per minimum wavelength at the excitation lines, or more. The best way to find a suitable sampling rate of the excitation is to choose one, to plot the excitation time series at these lines, to judge its spatial variability (caused by discontinuities, focal mechanism, etc.) and to sample most densely in the locations where more abrupt variations of the wave field take place. It is also important to note that the minimum shear wavelength of the *background* model is often larger than the minimum wavelength in the local structure under study, which permits a coarser sampling than in the FD caluclation. Examples of the excitation sampling are given below.

The DW-FD modeling then consists of two main steps. In the 1st step the background (1D) field due to a point source is computed, and complete seismograms are stored at the selected locations along the excitation lines. In this step the 1D model is, in principle, much larger (both horizontally and vertically) than the FD model. In the 2nd step the point source is no longer present and the medium is truncated to the FD domain. The prescribed solution from the 1st step serves as U_k. It is interpolated into the FD locations along the excitation lines. Thereafter, the FD calculations of U and U_r take place in domains A and B respectively. The results are plotted for predefined receivers as U and U_r, in domains A and B respectively. Or, if the U_k field was also stored at all the receivers in B, we compute $U = U_k + U_r$ there, and plot U everywhere.

An important feature of the present method is that the excitation lines form a box. It contrasts with the approach of FÄH *et al.* (1994), in which the FD region was subdivided into domains A and B by two vertical lines only. The advantage of using a box is that the FD domain can be made shallower. A more detailed explanation is given in ZAHRADNÍK (1995b), and is demonstrated below in the numerical examples. Another advantage of the excitation box is a better spatial sampling of the source radiation pattern. Finally, at least in some models, the residual field U_r is rather weak and thus more easily eliminated at the nonreflecting boundaries of the FD domain than the complete wave field U in the method of FÄH *et al.* (1994).

Verification of the Coupling Algorithm

Models investigated in this paper are schematically shown in Figure 2. Their specific features are given in Table 1. Only horizontal components are presented in this paper, and all of them are for the receivers at the free surface.

We present two numerical experiments to verify the coupling algorithm. In Experiment 1 an analytical solution is coupled with the FD calculation, while Experiment 2 consists in a FD-FD hybrid calculation. The actual DW-FD hybrid calculation will be presented in the next section.

Experiment 1 involves a homogeneous halfspace excited by an upward vertically propagating plane wave. This model is treated in two modes. Mode 1a assumes $U_k = U_{\text{inc}}$, where U_{inc} is the analytically prescribed incident wave field. Model 1b takes the analytically prescribed field $U_k = U_{\text{inc}} + U_{\text{ref}}$, where U_{ref} is the free-surface reflection of the incident wave. The excitation U_k is, in this model, computed and stored at all grid points and time levels required for the FD calculation. (For the FD grid steps, see Table 1.) The vertical segments of the excitation line b are located at $x = 40$ and 140 m. The horizontal segment is at $z = 28$ m. As the complete solution in both cases should be the same, $U = U_{\text{inc}} + U_{\text{ref}}$, we expect $U_r = U_{\text{ref}}$, and $U_r = 0$ for cases 1a and 1b respectively. As seen from Fig. 3, the expected result is actually obtained in Experiment 1b, but not in 1a. Model 1a is wrong not only in deriving $U_r \neq U_{\text{ref}}$, but also $U \neq U_{\text{inc}} + U_{\text{ref}}$. On the contrary, model 1b accurately provides $U_r = 0$ and $U = U_{\text{inc}} + U_{\text{ref}}$.

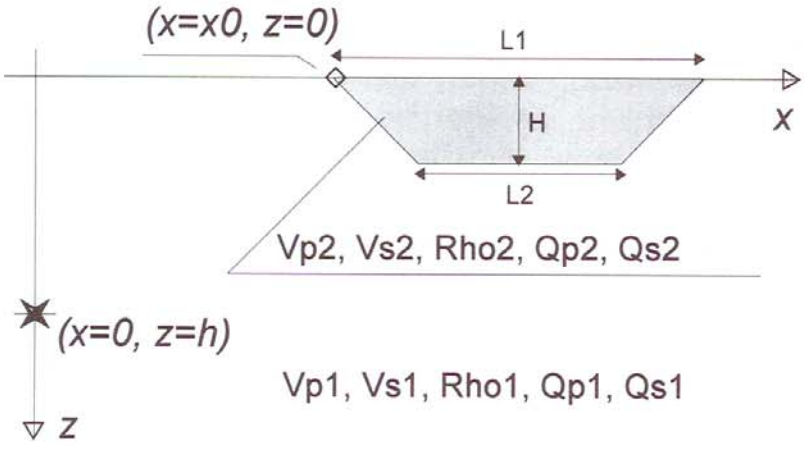

Figure 2

Schematic representation of the models ivnestigated in this paper. The excitation is by a point or line source at a depth h (asterisk) or by a plane wave. The background medium is a homogeneous halfspace. In some models a symmetrical basin is embedded in the halfspace. Its left corner is at $x = x0$, its width at the free surface is L1, and the bottom width is L2. The basin depth is H. The Vp, Vs, Rho, Qp and Qs denote the P- and S-wave velocities, density, and the P- and S-wave quality factors. For the particular models, see Table 1.

Table 1

Parameters of the investigated models. Here f_{max} is the maximum frequency generated by the source. The dx and dt are the FD grid steps. For explanation of the other symbols, see Figure 2

Experiment	Source	h (m)	f_{max} (Hz)	dx (m)	dt (s)	Vp1 (m/s)	Vs1 (m/s)	Rho1 (kg/m^3)	Qp1	Qs1
1a	plane wave $U_k = U_{inc}$	–	10	1	0.00086	–	700	1800	1000	1000
1b	plane wave $U_k = U_{inc} + U_{ref}$	–	10	1	0.00086	–	700	1800	1000	1000
2	line vert. force	60	6	1	0.0015	500	250	2000	100	100
3	point explos.	60	10	1	0.00086	700	350	1800	1000	1000
4	point disloc.	60	10	1	0.00086	700	350	1800	1000	1000
5	point explos.	60	10	1	0.00086	700	350	1800	1000	1000

Experiment	$x0$ (m)	L1 (m)	L2 (m)	H (m)	Vp2 (m/s)	Vs2 (m/s)	Rho2 (kg/m^3)	Qp2	Qs2
1a	–	–	–	–	–	–	–	–	–
1b	–	–	–	–	–	–	–	–	–
2	71	68	30	20	200	100	2000	15	10
3	–	–	–	–	–	–	–	–	–
4	–	–	–	–	–	–	–	–	–
5	849	78	40	20	200	100	1800	15	10

What brought about the failure in Experiment 1a? Prescribing the known wave field as $U_k = U_{inc}$ we, in fact, assume that the background medium is unbounded. Therefore, adding the free surface during the 2nd step of the hybrid method does not represent a purely local variation of the background model inside the excitation box. As it is only the excitation box where an interaction between the U_k and U_r takes place, and where the U_r can be generated, the box cannot guarantee a proper generation of the residual field U_r reflected from the free surface outside of the box. Certainly, due to the interaction at the excitation lines, the error in the residual field also penetrates inside, deteriorating the complete field there.

On the other hand, in Experiment 1b, where the prescribed field is $U_k = U_{inc} + U_{ref}$, the background medium is just the homogeneous halfspace. Consequently, in the 2nd step we do not add any heterogeneity, i.e., we only try to reproduce the background field. No sources of the residual field exist either inside or outside of the excitation box. Resultingly, we correctly obtain both $U_r = 0$ and $U = U_{inc} + U_{ref}$.

This experiment suggests a general rule that *all sources of the residual wave field should always be contained inside the excitation box*. In other words, the background model in the first step and the model used in the subsequent FD step cannot differ outside the excitation rectangle.

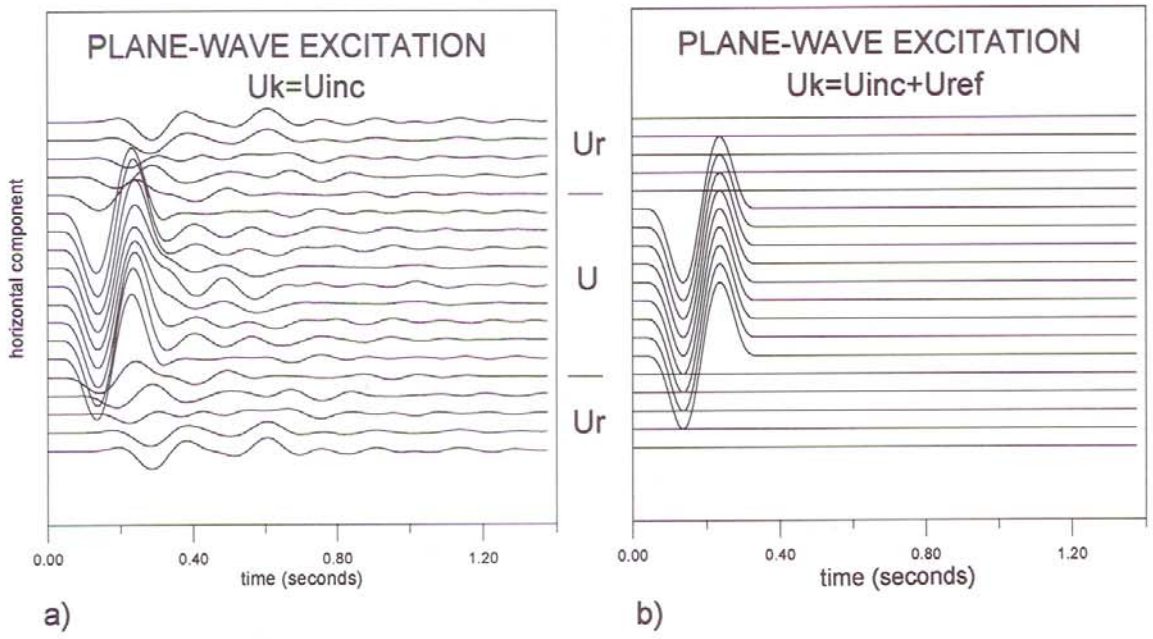

Figure 3

Hybrid analytic-FD synthetics for a homogeneous halfspace, excited by a vertically propagating **plane *S* wave**; Experiments 1a, b, Table 1. The free-surface time histories are plotted with a step of 10 m. Five curves at the top and five at the bottom display the residual field U_r in domain B. Those remaining present the complete field U in domain A. Panel a: the background field represented by the incident wave only. Panel b: the background field represented by the incident + reflected wave.

Remark: The only possible way of correctly securing the complete halfspace wave field $U_{\text{inc}} + U_{\text{ref}}$ in the excitation box in case of $U_k = U_{\text{inc}}$, would be to have the entire free surface of the FD model included inside the excitation box (domain A). This can be achieved by two *horizontal* excitation lines a and b. This is, of course, not new, since such a method has been intuitively used for a long time in our previous FD codes to simulate the incidence of plane waves onto the near-surface structures from below.

Experiment 2 illustrates the hybrid method based on coupling two FD calculations, i.e., the FD-FD method. The reason for starting from FD-FD, before studying DW-FD, is simplicity: using a line source in the first FD step, and a 2D model of the medium in both steps, the FD-FD case is purely two-dimensional.

A sedimentary basin is excited by a line source chosen in the form of a vertical body force (Fig. 4 and Table 1). In the 1st step the basin is not considered, i.e., the background medium is a homogeneous halfspace. The wave field generated by the source is calculated by the FD method and stored (in a form of the displacement time series) at two rectangular lines a and b. The vertical segments of the excitation line b are at $x = 59$ and 161 m, while the horizontal one is at $z = 32$ m. In this example the solution is stored in all FD grid points belonging to the excitation lines and at all time levels. Independently, the solution is also stored for selected receivers

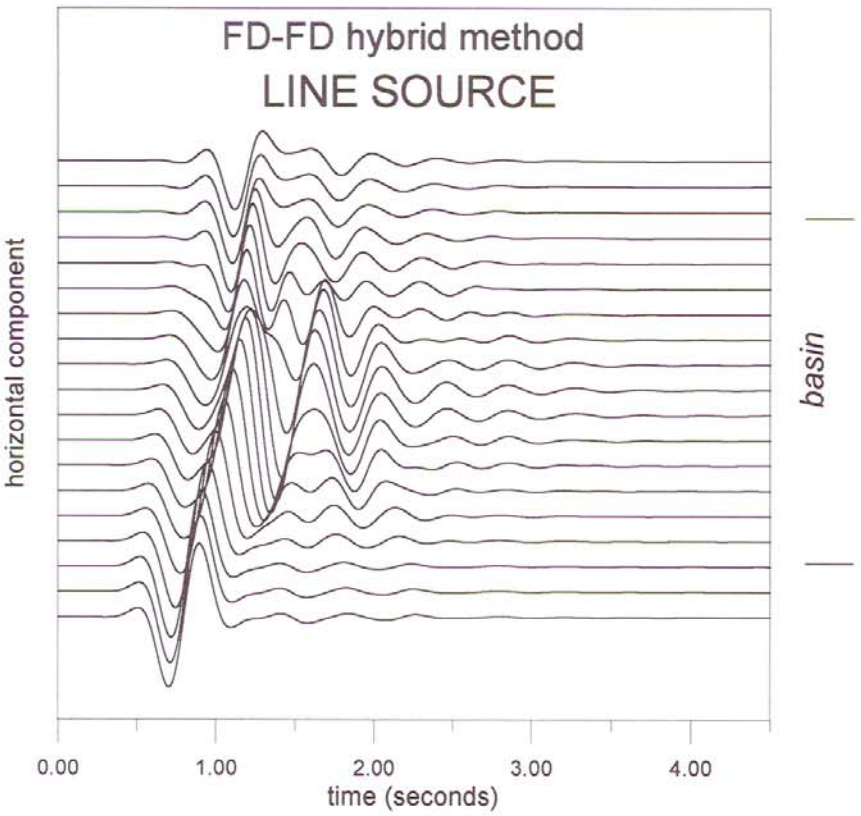

Figure 4
Hybrid FD-FD synthetics for a basin embedded in a halfspace, excited by a **line source** (**vertical force**); Experiment 2, Table 1. The complete field U is displayed for all receivers. The first receiver (bottom curve) is at $x = 60$ m, the others follow with the 5 m step. The hybrid FD-FD synthetics agree with those computed by the direct FD method within the width of line.

along the free surface for the subsequent plotting. In the 2nd step, the line source is switched off, and the basin is present inside the excitation box A. The FD calculation of U, and U_r, is performed in domains A and B, respectively. Finally, the complete wave field U is presented for the free-surface receivers. For that purpose the computed field inside the box is used directly (U) while outside the box the stored field U_k is added to the computed residual field U_r. The resulting seismograms are shown in Figure 4.

For comparison, this model is also solved directly by the FD method, including both the source and basin in a single FD run. (This is possible here because of the small size of the present test model.) These seismograms agree perfectly, within the width of line, with those previously obtained from the hybrid calculation.

Three features of the present successful test are to be emphasized: (i) The line source made the entire problem purely 2D. As shown later, point sources will yield more complications. (ii) The background (1st step) solution was a complete halfspace solution, not only the incident wave. Using the incident wave as U_k would

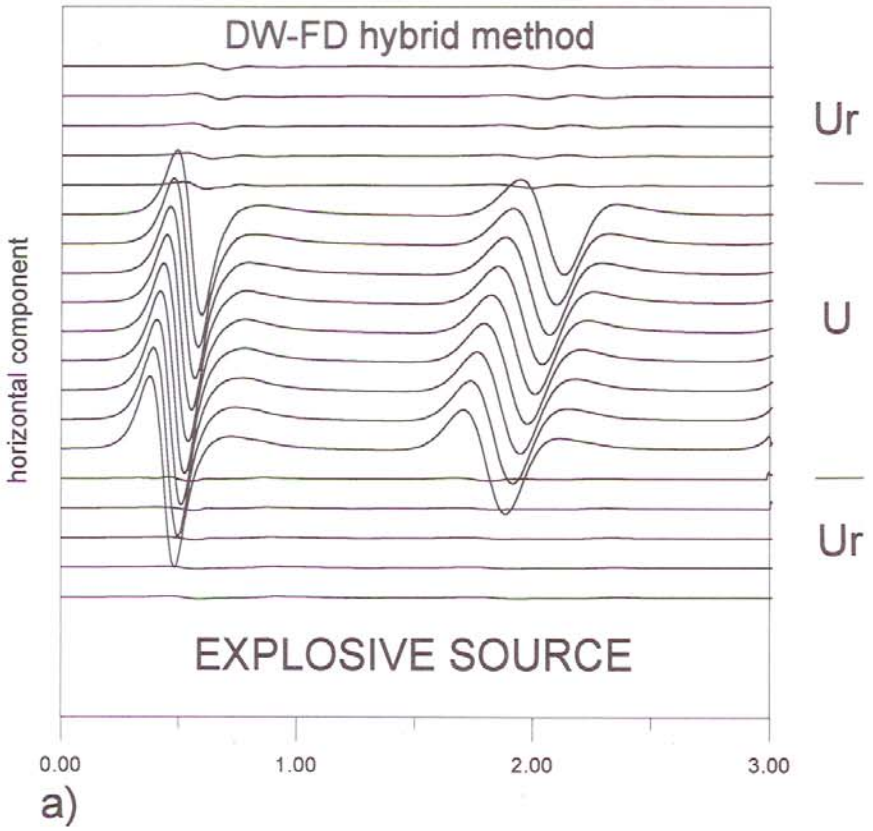
DW-FD hybrid method
Ur
U
Ur
horizontal component
EXPLOSIVE SOURCE
0.00
1.00
2.00
3.00
a)

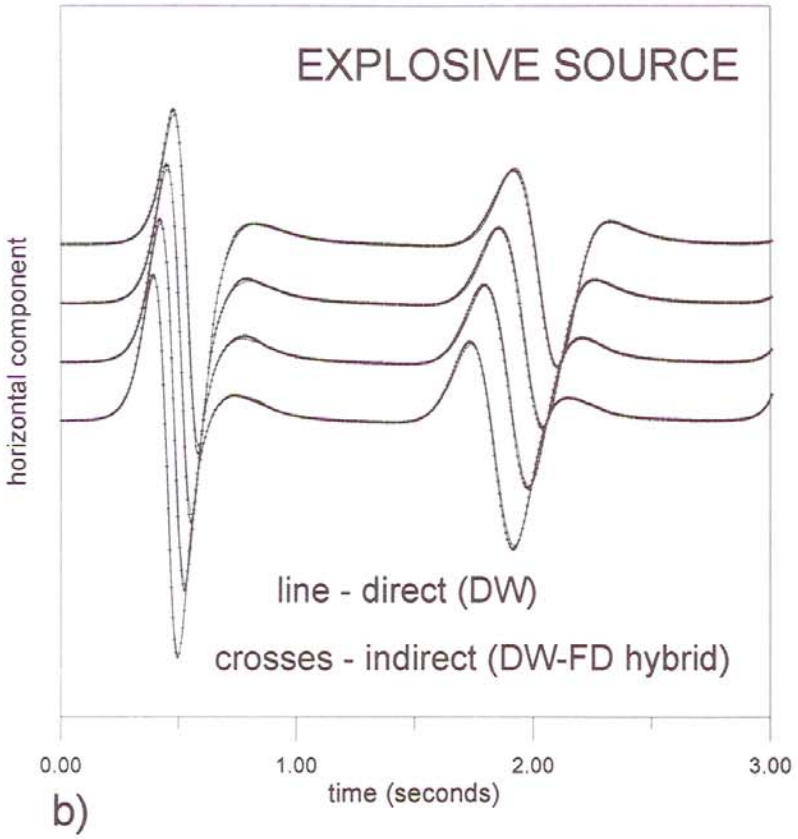
EXPLOSIVE SOURCE
horizontal component
line - direct (DW)
crosses - indirect (DW-FD hybrid)
0.00
1.00
2.00
3.00
time (seconds)
b)

yield erroneous results, as in Experiment 1a. (iii) Although the source was relatively deep, the excitation box was rather shallow.

DW-FD Verification in 1D Models

After successfully checking the coupling algorithm, we proceed to the key point of this paper; investigation of the DW-FD hybrid method. Its properties are illustrated in two examples in which the same 1D model of medium is used in the DW and FD calculations. It is possible to state that here we are interested only in a 'reproduction' of the DW solution by the FD method.

Experiments 3 and 4 treat the wave field in a homogeneous halfspace, excited by a point explosive and shear dislocation sources, respectively (Table 1). In both cases the source lies inside the FD plane. The seismic moment time variation is a 'smooth step' and the acceleration wave field is computed. The excitation rectangle has its outer segments (line *b*) at $x = 838$ and 938 m and at $z = 28$ m. In the 1st step the complete DW solution (including the free-surface effects) is stored at the excitation lines *a* and *b*. The sampling of these lines is coarser than in the subsequent FD model. It is performed at equal intervals of 8 m, both in the vertical and horizontal directions, and with a time step of 0.01172 s. It roughly corresponds to $\lambda_{\min}/4.4$, where $\lambda_{\min}$ is the minimum shear wavelength. In the 2nd step the point source is switched off while the excitation at lines *a* and *b* is on and the FD calculation of U and U_r in the domains A and B takes place, respectively, as explained above in connection with eq. (1). The resulting solutions U (inside the excitation box) and U_r (outside) are plotted in Figures 5a and 6a for Experiments 3 and 4, respectively. For comparison, a direct DW calculation is also performed and overlain with the former in Figures 5b and 6b.

As seen from Figure 5b, Experiment 3 with its point *explosive* source still gives a good agreement between the hybrid and direct solutions. A weak residual field for this model is present outside the excitation box (Fig. 5a).

For the *shear dislocation* point source in Experiment 4, the DW-FD hybrid result is much less accurate than in the explosive source case. This can be seen from comparing the hybrid and direct solutions in Figure 6. The residual field U_r is larger than in Experiment 3.

Theoretical explanation of Experiments 3 and 4 is as follows: The 2D elastic wave propagation is governed by two coupled equations which can be schematically

Figure 5

Hybrid DW-FD synthetics for a homogeneous halfspace, excited by a **point explosive source**; Experiment 3, Table 1. Panel a: The bottom time history is for $x = 798$ m, the others follow with the step of 10 m. Five curves at the bottom and five at the top present the residual field U_r. Those remaining are for the complete field U. Panel b: Comparison of the complete field U computed by the DW-FD hybrid method (crosses), and the direct DW method (line). The bottom seismogram is for $x = 858$ m, the others follow with the 20 m step.

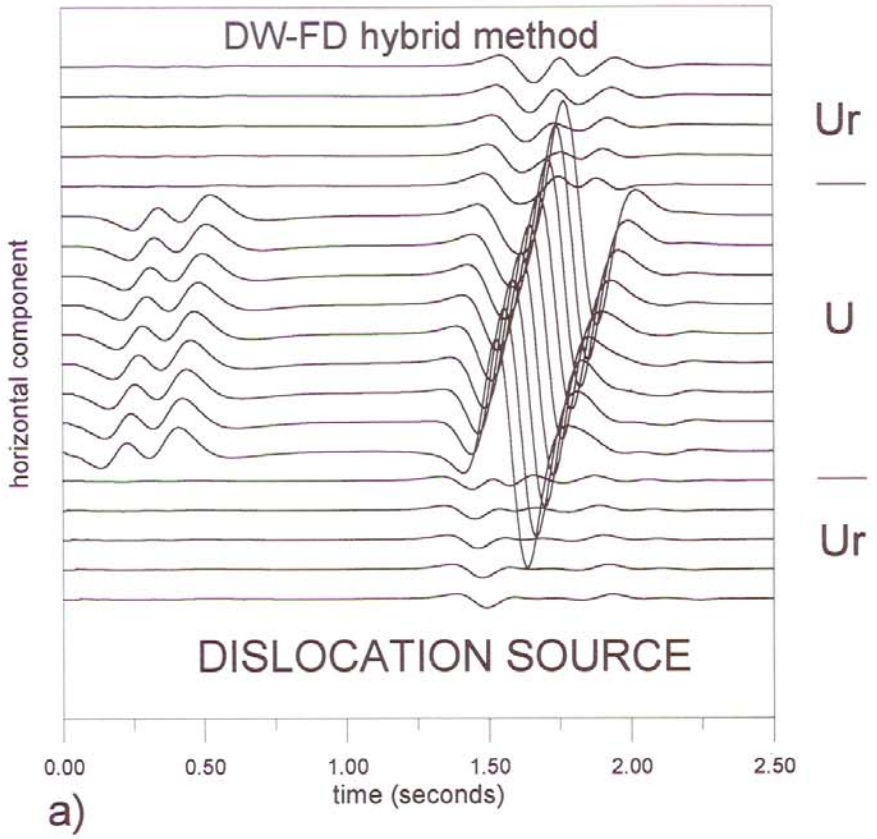
DW-FD hybrid method
Ur
U
Ur
horizontal component
DISLOCATION SOURCE
0.00
0.50
1.00
1.50
2.00
2.50
time (seconds)
a)

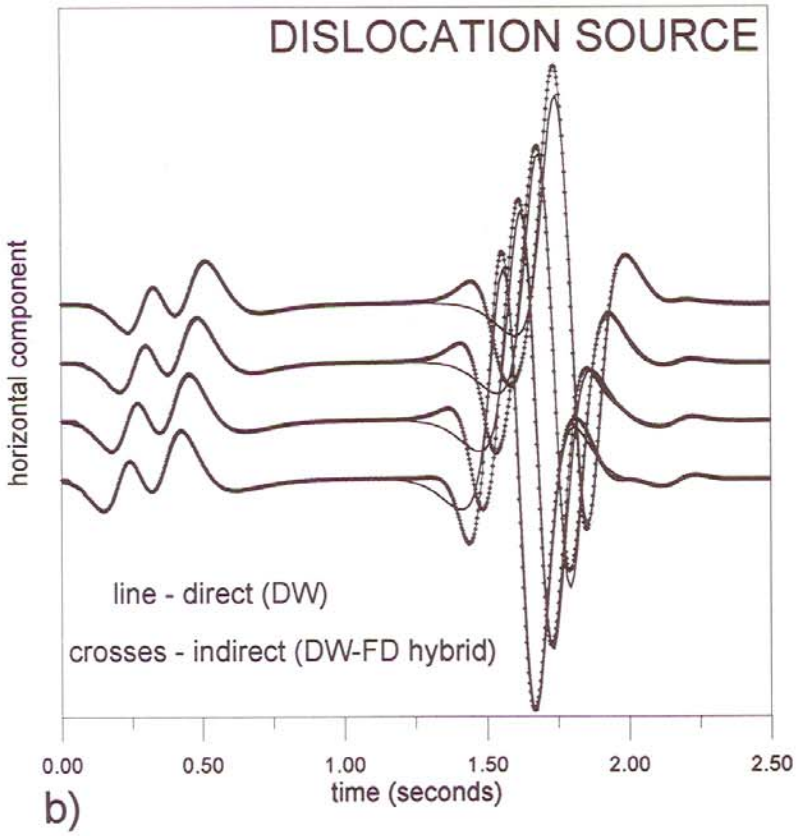
DISLOCATION SOURCE
horizontal component
line - direct (DW)
crosses - indirect (DW-FD hybrid)
0.00
0.50
1.00
1.50
2.00
2.50
time (seconds)
b)

written as

$$D1(u, w) = \ddot{u}, \tag{2a}$$

$$D2(u, w) = \ddot{w}, \tag{2b}$$

where $D1$ and $D2$ are the spatial differential operators involving the elastic parameters and density; and u and w denote the horizontal and vertical components of the displacement, parallel to the two in-plane coordinates x and z, respectively. At the same time, the 3D point-source case is described by three coupled equations, where in addtition to u and w, the transverse displacement component, v, also appears. It is parallel to the out-of-plane coordinate y. Two of the 3D equations, namely those updating u and w, read

$$D1(u, w) + \partial f1(u)/\partial y + \partial g1(v)/\partial y = \ddot{u}, \tag{3a}$$

$$D2(u, w) + \partial f2(w)/\partial y + \partial g2(v)/\partial y = \ddot{w}. \tag{3b}$$

Here $D1$ and $D2$ are the same differential operators as in equation (2), while $f1$, $g1$, $f2$, and $g2$ represent spatial differential operators involving the elastic parameters and the displacement components u and v, as indicated in the brackets.

For the 3D point *explosive* source, the transverse displacement component vanishes, $v = 0$, hence also the terms $\partial g1(v)/\partial y$ and $\partial g2(v)/\partial y$. Therefore, in the 3D explosion case, the two equations of motion for u and w differ from the 2D equations only in the terms $\partial f1(u)/\partial y$ and $\partial f2(w)/\partial y$. Physically it means that the 3D wavefront spreading takes place, although the wave field stays the same in any vertical plane containing the source. If, moreover, the explosive source is relatively distant, the terms $\partial f1(u)/\partial y$ and $\partial f2(w)/\partial y$ are small. Conversely, in a general 3D case, e.g., that of the point *dislocation* source, not only the 3D wave front spreading takes place, also the nonspherical radiation pattern prevents the decoupling of u and w from v, as represented by the terms $g1$ and $g2$. This interpretation explains the differences observed between Experiments 3 and 4: the good agreement between the DW-FD hybrid and the direct DW results for the point explosive source and the discrepancies between the two solutions for the dislocation source. However, even in the dislocation case, the P wave still has $v = 0$. That is why, in Figure 6, the P-wave group features a better agreement between the DW-FD and DW solutions than the S-wave group (with $v \neq 0$).

Figure 6

Hybrid DW-FD synthetics for a homogeneous halfspace, excited by a **point shear dislocation source** (strike 115, dip 80, rake 167); Experiment 4, Table 1. Panel a: The bottom time history is for $x = 798$ m, the others follow with the step of 10 m. Five curves at the bottom and five at the top present the residual field U_r. Those remaining are for the complete field U. Panel b: Comparison of the complete field U computed by the DW-FD bybrid method (crosses) and the direct DW method (line). The bottom seismogram is for $x = 858$ m, the others follow with the 20 m step.

In other words, the 3D-varying wave field from the DW calculation is not easily forwarded into the 2D FD calculation even if the model of the medium remains only 1D in both the DW and FD steps. The larger the 3D variation (e.g., larger for the dislocation source than for the explosive one, or larger for a less distant source), the larger the inconsistency of the 3D solution with the 2D model. Hereafter, we shall refer to it simply as the '3D-2D inconsistency'. Naturally, if the point source was located off the FD plane, this inconsistency would be even larger. The latter case is not treated in this paper, however see also ZAHRADNÍK (1995b), where a method for improving the propagation of the 3D excitation in the 2D models has been suggested.

The main results of this section, that starting from a non-separable 3D solution (u, v, w), and trying to 'continue' such a solution in a 2D model we never accomplish correctly (u, v), can be explained also in analogy with Experiment 1. Experiment 1 suggests that no correct hybrid result can be expected once the background and the FD model differ outside the excitation box. In Experiments 3 and 4 the situation is, in fact, similar. Although considering the same 1D model of the medium, the DW point source calculation is 3D, however the FD calculation is 2D. Therefore, the difference between the DW and FD wave fields exists everywhere. And, this is precisely the reason why, specifying a 3D excitation at the 2D box, neither U_r nor U can be obtained quite accurately.

How will the 3D-2D inconsistency affect the 2D models with local heterogeneities? What we obtain from the FD step is a certain approximation to (u, w), say $(\bar{u}, \bar{w}) \doteq (u, w)$. The quality of this approximation depends on the 3D variation of the DW solution. However, importantly, this FD solution $(\bar{u}, \bar{w})$ is already satisfying the 2D equations of motion (2). It is *reproducible* in the 2D model: For example, if we store the solution $(\bar{u}, \bar{w})$ on the excitation lines and use it as the excitation in the unchanged 2D model, we obtain again the same field $(\bar{u}, \bar{w})$ inside the excitation box and the zero residual field outside (as numerically verified but not shown here). As a consequence, the 3D-2D inconsistency should not increase further in the second step, during which a localized 2D heterogeneity is placed in the excitation box. Simply speaking, the error originating from the 3D-2D inconsistency is made 'only once'. The wave propagation inside a localized 2D heterogeneity should not further increase this error. To prove it numerically a 2.5D method is needed, in which a point source radiation and a 2D heterogeneity are treated accurately (e.g., PEDERSEN *et al.*, 1994).

DW-FD Application in a 2D Model

Finally we proceed to the DW-FD calculation in which the solution from the 1st (DW) step is used to excite a localized 2D heterogeneity, included in the excitation box during the 2nd (FD) step.

Experiment 5. The model is presented in Figure 2 and Table 1. It consists of a sedimentary basin embedded in an otherwise homogeneous halfspace. As in the previous section, an in-plane point source is assumed. As the 3D-2D inconsistency was found above for the dislocation source, we consider the case in which the excitation is performed by a relatively distant explosive source. The position of the excitation box, as well as its spatial and temporal samplings, is identical to Experiments 3 and 4. As compared to Experiments 3 and 4, the same source time function is used but the displacement (not the acceleration) is computed. For this reason, and also because both the DW and FD methods correctly describe the near-field source contributions, the resulting seismograms feature a significant static displacement (Fig. 7). That is why this result is an interesting combination of two effects: the near-field source effect and the local site effect. As the static displacement is basically a low-frequency phenomenon, it remains nearly untouched by the shallow basin as compared to the background model. However, added to the background solution is a considerable complexity of the high-frequency wave-field components, caused by 2D multiple reflections inside the basin. At the same time,

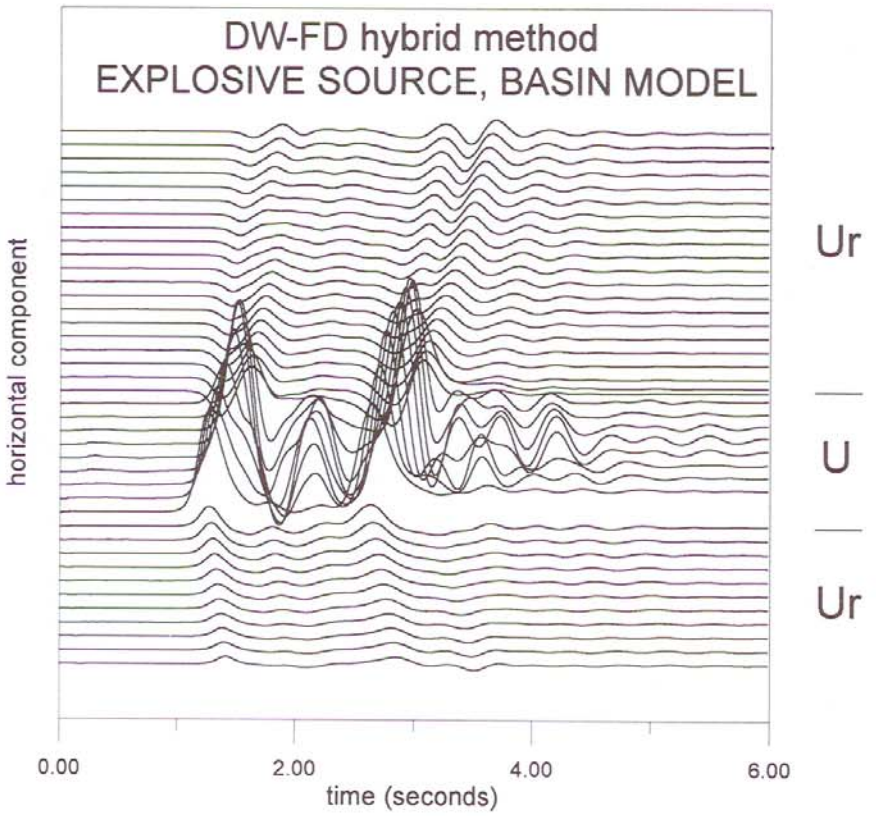

Figure 7

Hybrid DW-FD synthetics for a basin embedded in a halfspace, excited by a **point explosive source**; Experiment 5, Table 1. The bottom time history is for $x = 738$ m, the others follow with the step of 10 m. Eleven curves at the bottom and twenty at the top display the residual field U_r outside of the basin. Those remaining represent the complete field U at the surface of the basin.

outside of the basin the wave field is less changed, compared to the background. In particular, the backward scattered waves are rather weak.

Joint investigations of the near-field source effects, and the site effects, have been rather rare to date. Most published works have either concentrated on the site effects in the far-field approximation or on the complete source effects without detailed analyses of the site effect. This is why we believe that the DW-FD hybrid method will find practical applications in the ground-motion assessment at such sites where low-frequency engineering structures (such as long bridges, high-rise buildings, etc.) might be damaged by static displacements, and, at the same time, some of their structural components are vulnerable to the relatively high-frequency motions affected by the local site geology.

Of course, for applications like these, the finite source extent should be considered. With regards to the DW method, this can be achieved by summing point source subevents. The DW-FD coupling algorithm developed in the present paper could thus be applied to extended sources such as earthquake faults.

Another alternative, introducing not only the finite-extent sources, but also perhaps more realistic path effects, would be to treat the source and path by a stochastic method, for example, as in ROVELLI *et al.* (1994).

Conclusion

A new method has been developed which is useful in treating efficiently seismic wave fields at localized 2D near-surface structures embedded in a 1D (horizontally layered) background medium and excited by a point source. It is a hybrid method in which the background model is solved by the DW method, the local 2D structure by the FD method, and their coupling is realized on a rectangular excitation box surrounding the local structure from the left, right and bottom sides. Using the DW method has proved advantageous because the background wave field is described quite completely, including the near-field source effects also, e.g., the residual static displacements.

Although our main objective has been to develop software for applications in earthquake seismology, in this paper we focused on important 'technical' aspects of the method. This resulted in the following findings:

(i) The wave field U must be decomposed in $U_k + U_r$ in such a way that U_k, the known background field, is available at the excitation lines throughout the entire investigated time window, and all sources of the residual field U_r are within the excitation box only. In other words, the background DW structural model and the final FD model should not differ outside the excitation box.

(ii) Wave fields due to relatively distant 3D explosive point sources, located in the same plane as that of the FD model, can be propagated through 2D FD models with little distortion. This results because the inconsistency between the

3D DW solution and the 2D FD solution in that case derive from the 3D spreading only.

(iii) Radiation from the dislocation point sources, in particular their S waves, is more sensitive to the 3D-2D inconsistency than the explosive point-source wave field. This is due to the fact that the 2D calculation does not reproduce the coupling between the in-plane and out-plane displacement components.

The main test example of this paper (Experiment 5, Fig. 7) has proved the usefulness of the method when studying the ground motion in a sedimentary basin. The response displayed not only a considerable site effect, but also a static displacement due to the near-field source effect.

The advantages of the suggested DW-FD hybrid method, compared to the direct FD solution, are evident. Any direct FD model comprising the source, path, and site would require considerably more computation time and memory resources, even if spatially irregular grids and higher-order schemes were used. Moreover, the methods currently available for including the point sources in the 2D FD calculations are the far-field approximations only.

Possible application areas of the present method in *earthquake seismology* are problems in which source, path and site effects must be treated as a whole. Mostly it will apply to situations in which engineering structures such as long bridges or high-rise buildings might be damaged by low frequency ground motions, including the static displacements, while, at the same time, some of their structural components are vulnerable to the relatively high-frequency motions affected by the local site geology. Further generalizations of the DW-FD method should include the nonlinear stress-strain relations, at least in the FD step, wherever strong ground motions in loose soils are to be treated properly.

In *exploration seismology* the ground-roll effects, caused by near-surface layers, often obscure reflections from deeper horizons. These effects, in particular those of laterally varying near-surface structures, can also be treated by the present method.

Acknowledgments

The authors thank O. Coutant (Joseph Fourier University, Grenoble) for kindly providing his DW code, F. Hron (Alberta University, Edmonton) for critical reading of the manuscript, and J. Kristek (Slovak Academy of Sciences, Bratislava) for performing part of the computations. Thanks are also extended to H. Gärtner (Geophysik GGD, Leipzig) for valuable comments regarding possible applications in the seismic exploration. Careful reviews by anonymous reviewers aided our improvement of the presentation and are gratefully acknowledged. This work was financially supported from the Charles University grant GAUK-321, the Czech Republic grant GAČR-0507, the NATO ENVIR.LG 940714 grant, and the NATO Science for Stability GR-COAL grant.

REFERENCES

ABOUDI, J. (1971), *Numerical Simulation of Seismic Sources*, Geophysics *36*, 810–821.

ALTERMAN, Z. S., and KARAL, F. C. (1968), *Propagation of Elastic Waves in Layered Media by Finite Difference Methods*, Bull. Seismol. Soc. Am. *58*, 367–398.

BOUCHON, M. (1981), *A Simple Method to Calculate Green's Functions for Elastic Layered Media*, Bull. Sesimol. Soc. Am. *71*, 959–971.

EMMERICH, H. (1992), *PSV-wave Propagation in a Medium with Local Heterogeneities: A Hybrid Formulation and its Application*, Geophys. J. Int. *109*, 54–64.

EMMERICH, H., and KORN, M. (1987), *Incorporation of Attenuation into Time-domain Computations of Seismic Wave Fields*, Geophysics *52*, 1252–1264.

FÄH, D., SUHADOLC, P., MUELLER, St., and PANZA, G. F. (1994), *A Hybrid Method for the Estimation of Ground Motion in Sedimentary Basins: Quantitative Modeling for Mexico City*, Bull. Seismol. Soc. Am. *84*, 383–399.

KENNETT, B. L. N., and KERRY, N. J. (1979), *Seismic Waves in a Stratified Half Space*, Geophys. J. R. Astr. Soc. *57*, 557–583.

KUMMER, B., BEHLE, A., and DORAU, F. (1987), *Hybrid Modeling of Elastic-wave Propagation in Two-dimensional Laterally Inhomogeneous Media*, Geophysics *52*, 765–771.

MOCZO, P., and BARD, P.-Y. (1993), *Wave Diffraction, Amplification and Differential Motion near Strong Lateral Discontinuities*, Bull. Seismol. Soc. Am. *83*, 85–106.

PEDERSEN, H. A., SANCHEZ-SESMA, F J., and CAMPILLO, M. (1994), *Three-dimensional Scattering by Two-dimensional Topographies*, Bull. Seismol. Soc. Am. *84*, 1169–1183.

ROVELLI, A., CASERTA, A., MALAGNINI, L., and MARRA, F. (1994), *Assessment of Potential Strong Ground Motions in the City of Rome*, *Annali di Geofisica 37*, 1745–1769.

VAN DEN BERG, A. (1984), *A Hybrid Solution for Wave Propagation Problems in Regular Media with Bounded Irregular Inclusions*, Geophys. J. R. Astr. Soc. *79*, 3–10.

VIDALE, J. E., and HELMBERGER, D. V. *Path effects in strong motion seismology*. In *Methods of Computational Physics 11* (ed. Bolt B.) (Academic Press, New York 1987) pp. 267–319.

ZAHRADNÍK, J., (1995a), *Simple Elastic Finite-difference Scheme*, Bull. Seismol. Soc. Am. *85*, 1879–1887.

ZAHRADNÍK, J. (1995b), *Comment on 'A Hybrid Method for the Estimation of Ground Motion in Sedimentary Basins: Quantitative Modeling for Mexico City'* by Fäh *et al.*, Bull. Seismol. Soc. Am. *84*, 383–399, 1994, Bull. Seismol. Soc. Am. *85*, 1268–1270.

ZAHRADNÍK, J., and PRIOLO, E. (1995), *Heterogeneous Formulations of Elastodynamic Equations and Finite-difference Schemes*, Geophys. J. Int. *120*, 663–676.

ZAHRADNÍK, J., MOCZO, P., and HRON, F. (1993), *Testing Four Elastic Finite-difference Schemes for Behaviour at Discontinuities*, Bull. Seismol. Soc. Am. *83*, 107–129.

(Received July 10, 1995, revised November 11, 1995, accepted January 22, 1996)